Available online at www.sciencedirect.com
SCIENCE DIRECT
Journal of Catalysis 240 (2006) 194–202
JOURNAL OF CATALYSIS
www.elsevier.com/locate/jcat

About the octopus-like growth mechanism of carbon nanofibers over graphite supported nickel catalyst

Cuong Pham-Huu [a,*], Ricardo Vieira [a,b], Benoit Louis [a], Alain Carvalho [c], Julien Amadou [a], Thierry Dintzer [a], Marc J. Ledoux [a]

[a] *Laboratoire des Matériaux, Surfaces et Procédés pour la Catalyse, UMR 7515 du CNRS, ECPM, Université Louis Pasteur, 25, rue Becquerel, 67087 Strasbourg cedex 02, France*

[b] *Laboratorio de Combustão e Propulsão, Instituto Nacional de Pesquisas Espaciais, Rodovia Presidente Dutra Km 40, 12630-000 Cachoeira Paulista - SP, Brasil*

[c] *GEMME, IPCMS, UMR 7504 du CNRS, 23, rue du Loess, 67037 Strasbourg cedex 08, France*

Received 13 January 2006; revised 17 March 2006; accepted 19 March 2006

Available online 27 April 2006

Abstract

Carbon nanofibers (CNFs) with a uniform diameter of ca. 30 nm and a productivity of 50 $g/(g_{Ni}\,h)$ were grown by catalytic decomposition of a C_2H_6/H_2 mixture over a nickel (1 wt%) catalyst supported on graphite microfibers, which constitutes the macroscopic shape of the final C/C composite. The catalyst particle size and dispersion before CNF growth was characterized by high-resolution scanning electron microscopy (SEM). The resulting composite consisting of a weblike network of CNFs covering the starting catalyst was characterized by SEM and transmission electron microscopy to gain more insight into the relationship between the starting nickel catalyst particles and the as-grown CNFs. Apparently, CNF growth proceeds from different mechanisms: a base-growth mechanism, involving especially the large nickel particles; a tip-growth mechanism, involving mostly the smaller nickel particles; and a tip/octopus-growth mechanism (the most common), involving all particles. In all cases, restructuring of the nickel particle from a globular to a more faceted structure seems to be the key step in producing an extremely large quantity of CNFs with yields up to 100 wt%.

Keywords: Carbon nanofibers; CVD; Macroscopic shape; Growth mechanism; Octopus growth

1. Introduction

Carbon nanotubes and nanofilaments are cylindrical or tubular carbon formation with radii on the nanometer scale and lengths of up to several micrometers [41,42]. The primary difference between a nanotube and a nanofiber is the orientation of graphite basal planes with respect to the axis. In carbon nanotubes, the graphene sheets are oriented in concentric layers along the longitudinal axis, thus exposing basal planes of graphite. In carbon nanofibers (CNFs), the graphene sheets are oriented in a conic arrangement (i.e., Chinese hat) along the fiber axis, with exclusively prismatic planes exposed.

CNFs have been thoroughly studied over the last decade, especially for their use as a catalyst support displaying high activity and peculiar selectivity compared with traditional catalysts, thus making them attractive compared with alumina, silica, or activated charcoal [1–6]. Metal catalysts supported on CNFs or nanotubes exhibit unusual activity and selectivity patterns compared with those seen with the traditional catalyst supports [7–11]. The absence of micropores displayed by these nanoscale materials significantly reduces mass transfer limitations, especially in liquid-phase reactions [12,13]. The peculiar interactions between the deposited metallic phase and the exposed planes of the support, leading to the formation of active metallic faces [14–16], were advanced to explain the observed catalytic results. The pioneering work done by Planeix et al. and Baker and coworkers has opened new routes for tailoring the properties of nanoscopic carbon through changing the orientation of the graphite platelet stacks, hence altering the interactions between the deposited active phase and the carbon support [14,15].

* Corresponding author.
E-mail address: cuong.lcmc@ecpm.u-strasbg.fr (C. Pham-Huu).

0021-9517/$ – see front matter
doi:10.1016/j.jcat.2006.03.017

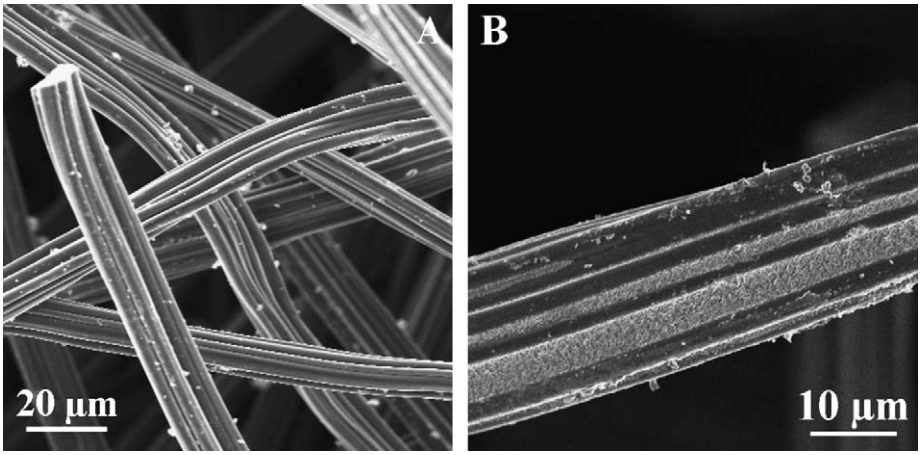

Fig. 1. SEM images of the starting graphite felt which was constituted by a closely packed network of micrometers graphite filaments (A) with a smooth surface (B).

But these materials have been usually synthesized in the form of a nanoscopic powder, making their handling and large-scale use hazardous, especially in fixed-bed catalytic reactions. The handling of the carbon nanostructures is hampered by the formation of fine particles, leading to a high-pressure drop along the catalyst bed. Consequently, it is of interest to identify new methods to allow the synthesis of carbon nanostructures in a larger scale along with direct macroscopic shaping for their subsequent use as catalyst supports in the field of heterogeneous catalysis. It is expected that the macroscopic shaping of such nanostructured material will open opportunities for its use as a catalyst support compared with what is usually obtained on traditional catalyst supports [17,18]. De Jong's group has been very active in this field, preparing macroscopic shapes consisting of CNFs strongly anchored on millimeter-sized supports [43]. Supporting CNFs with macroscopic shape and tortuosity have been synthesized by Lefferts et al. [44] who used metallic foam as the starting macroscopic host structure.

The macroscopic support should not alter the physical properties of the carbon nanostructures deposited on it, that is, high mechanical strength to avoid breaking and catalytic bed plugging; high specific volume, to afford a high space velocity of the gaseous reactants; high thermal conductivity, which is a required condition for a practical use in highly exothermic or endothermic processes; and, finally, high chemical resistance, to allow used in aggressive environments (i.e., highly acidic or basic media). Furthermore, the support should also provide an electronic interaction with the deposited phase or the contact surface between the active phase and the gaseous reactant mixture, which significantly increases the activity toward the production of CNFs compared with that observed on bulk catalytic material. Among the different supports used, carbon as a carrier material seems the most promising because of its light weight, high chemical resistance, and good thermal conductivity.

The present article proposes a mechanism of CNF growth, that is, base growth and/or tip growth depending on the catalyst particle size, leading finally to an octopus-like formation of CNFs from a single nickel particle. Our results indicate that adequation between the diameter of the CNFs produced and the size of the starting catalyst particle did not occur, because CNFs with a homogeneous diameter of ca. 30 nm were grown from a single nickel particle larger than 100 nm.

2. Experimental

A macroscopic carbon felt disk (3 cm diameter, 0.5 cm thick) with a smooth external surface (Figs. 1A and B) supplied from Carbone Lorraine Co., with a specific surface area of 1 $m^2\,g^{-1}$, was impregnated with 1 wt% of nickel by incipient wetness impregnation using a solution of ethanol and water. Before impregnation, the macroscopic carbon felt was treated in concentrated HNO_3 (37 vol%) at room temperature overnight to increase the amount of anchoring sites on the low-reactive basal planes of graphite. de Jong et al. [19] have reported that the nature of the carbon surface can be modified at will by introducing oxidic groups such as carboxylic (–COOH), carbonyl (–CO), and hydroxylic (–OH) groups by means of acidic treatments, leading to a change in affinity for liquids. The material was subsequently used as a catalyst for CNF growth [12]. The as-impregnated solid was allowed to dry at 110 °C overnight and then calcined in air at 350 °C for 2 h to decompose the nickel salt into the corresponding nickel oxide. Separate TPO experiments carried out under similar conditions have demonstrated the near-complete absence of extensive carbon support oxidation during the oxidative treatment at 350 °C. The solid was then reduced in situ in flowing hydrogen at 400 °C for 2 h. The complete reduction of the nickel phase was verified by powder X-ray diffraction (result not shown).

The growth process was carried out on the reduced catalyst in a tubular quartz reactor (diameter, 30 mm; length, 600 mm) at atmospheric pressure in the presence of a mixture of ethane and hydrogen (total flow rate, 20 and 100 mL min^{-1}) at 680 °C. The reaction conditions were determined by an experimental design process providing the highest yield of CNFs (i.e., 100 wt%), along with an acceptable specific surface area for subsequent catalytic use (i.e., $>90\ m^2\,g^{-1}$).

Scanning electron microscopy (SEM) was performed using a Jeol F-6700 FEG microscope. Before observation, the sample was coated with a thin layer of gold to avoid the problems

of charge effect. BET surface areas were measured using a commercial BET unit (Coulter SA 3100, Coultronic SA) using N_2 adsorption at 77 K. Before the N_2 adsorption, samples were heated at 300 °C for 2 h under dynamic vacuum to desorb surface impurities. S_{BET} is the surface area of the sample calculated from the nitrogen isotherm using the BET method. Micropore surface area and pore volume were calculated using the *t*-plot method. The microstructure of the as-synthesized CNFs was investigated by transmission electron microscopy (TEM) on a Topcon 002B model working at 200-kV accelerating voltage with a point-to-point resolution of 0.17 nm. The sample was previously grounded and dispersed in an ethanolic solution. A drop of the solution was deposited on a copper grid covered with a holey carbon membrane.

Thermogravimetric analysis (TGA) was carried out on a SETARAM at a heating rate of 15 °C/min from room temperature up to 800 °C. The sample was mounted horizontally and purged with synthetic air (50 mL/min).

3. Results and discussion

3.1. Ni-supported graphite felt catalyst

Fig. 2 shows an SEM image of the nickel-supported catalyst after reduction in flowing hydrogen at 400 °C for 2 h. The nickel particles were loosely aggregated together to form larger particles on the graphite filament of size >100 nm. The relatively low dispersion of the nickel particles was attributed to the weak interaction between the graphite microfilament surface (i.e., basal plane with a hydrophobic character [20]) and the nickel salt precursor. The specific surface area of the sample remained almost unchanged at around 1 $m^2\,g^{-1}$, indicating that the graphite microfilament surface was not modified by the deposited nickel during the calcination and reduction steps, in agreement with the low nickel dispersion observed on SEM.

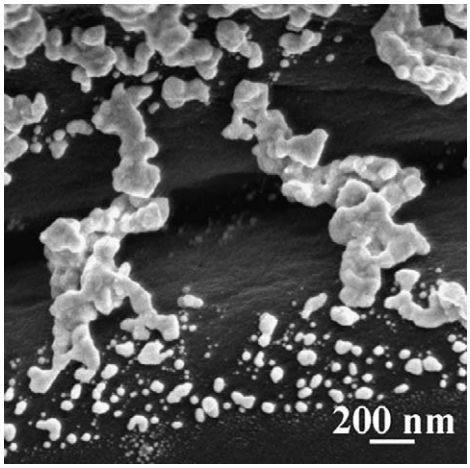

Fig. 2. SEM image of the Ni/graphite felt catalyst after calcination and reduction at 400 °C. Note the relatively low dispersion of the nickel particles on the microfilaments leading to an average particle size of about 100 nm.

3.2. CNF composite characteristics

The CNF yield obtained after 2 h of synthesis was close to 100 wt%, that is, 50 $g_{CNF}/(g_{Ni}\,h)$, taking into account the initial nickel loading of 1 wt%. A yield >100 wt% could be obtained while increasing the duration of synthesis. But at these higher yields, the mechanical anchorage of the fibers on the macroscopic host structure becomes weaker, and some nanofiber loss has been observed after sonication treatment. Note that the CNF yield obtained in the present work is among the highest yields reported in the literature to date.

The presence of H_2 inside the reactant mixture was essential to obtain regular, thin CNFs. In the absence of H_2, these nanofibers became less homogeneous with the appearance of irregular structures and nanoparticles. Similar results have also been reported by Van der Wal and Hall [21] during the synthesis of carbon nanotubes on a metal grid support using a mixture of C_6H_6 and C_2H_2, along with the presence or absence of hydrogen in the flow. Apparently, during CNF formation, hydrogen allows saturation of the graphite edges, preventing the formation of amorphous carbon. Park and Keane [22] observed that the structural arrangement within the CNFs was enhanced while increasing hydrogen content in the feed. In the presence of hydrogen, the faceting of the nickel catalyst was more pronounced, leading to the formation of a more well-ordered CNF structure [23,24]. The strong dependence of CNF yield and morphology on the crystallographic planes of the metal catalyst has already been reported by Goodman et al. [25]. The presence of H_2 also prevents carbon build-up on the nickel surface, which can ultimately lead to catalyst deactivation. However, the H_2 concentration should be low enough to prevent surface carbon removal by the combination and promotion of CH_4, which would have a negative impact on CNF yield.

The high yield observed was attributed to the break up of nickel oxide particles during the calcination process, which expose faceted structures by lattice dislocations and pit and crevice formation. In addition, on reduction in flowing H_2 at 400 °C, the remaining lattice structure of the oxide particles underwent breakup along the grain boundaries, leading to the formation of small metal particles. The highly defective structure of the final nickel metal probably played an important role in the quantity of CNFs produced. During growth, the nickel surface would be expected to become carburized by the reactant mixture, and thus the carburization rate would be expected to be higher in the presence of surface defects. Ting and Liu [26] suggested that during synthesis, nickel is carburized into NiC (at least superficially), with a *fcc* structure that allows the subsequent growth of multiple CNFs from Ni(111) planes, leading to the formation of an octopus-like CNF structure. The nickel crystallographic face reconstruction can be induced during CNF precipitation. The exact roles of the different crystallographic metal or carbide surfaces on CNF growth remain to be clarified. Similar results concerning the high yield of CNFs over nickel supported on carbon catalyst have recently been reported by Park and Keane [27].

Fig. 3A shows the morphology of the carbon nanoscopic/macroscopic composite after synthesis at 680 °C as observed

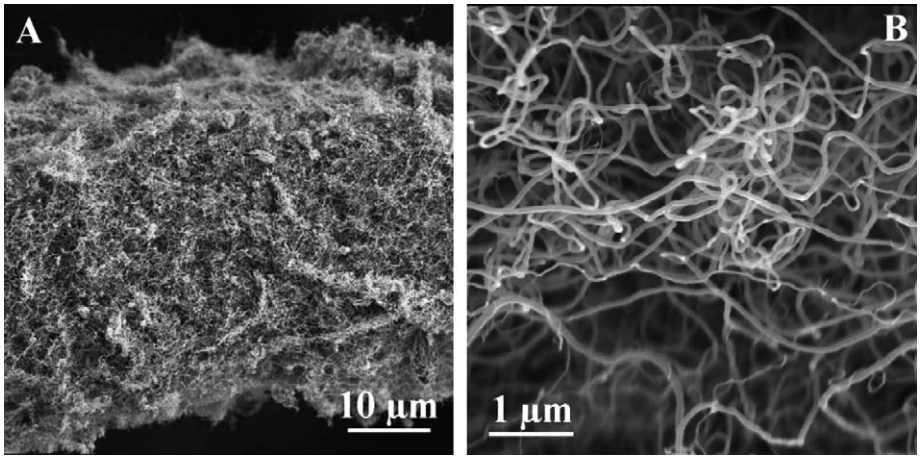

Fig. 3. SEM images of the final carbon nanofibers/graphite felt composite showing the complete coverage of the macroscopic host by a dense carbon nanofibers network (A). High-resolution SEM image showing the extremely homogeneous diameter of the carbon nanofibers, i.e., 30 nm (B).

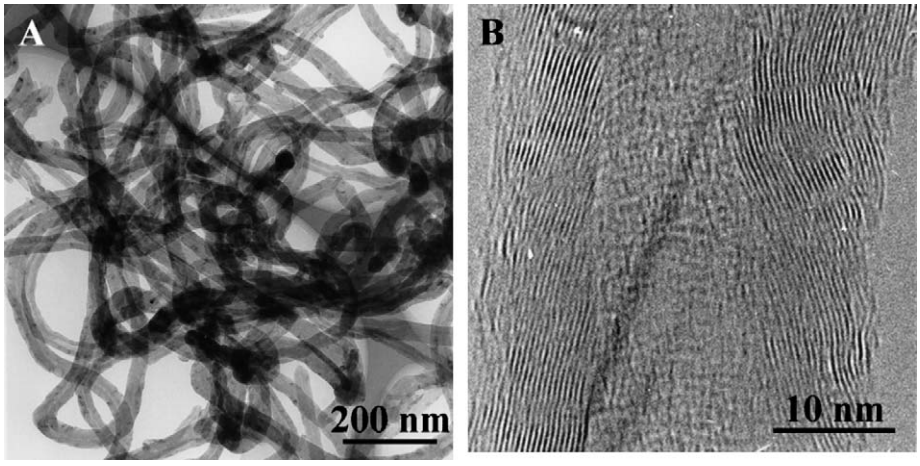

Fig. 4. Low magnification TEM image of the carbon nanofibers with an average diameter of around 30 nm (A). High-resolution TEM image showing the fishbone arrangement of the graphene planes along the fiber axis (B). The small amount of amorphous carbon observed on the outer surface can be attributed to the cooling effect during which amorphous carbon was built-up.

by SEM. The entire surface of the starting graphite filaments is covered by a dense network of CNFs of homogeneous diameter. The CNFs are entangled and have an average diameter of ca. 30 nm and a length of up to several micrometers, according to the high-magnification SEM image (Fig. 3B). The homogeneous average diameter of the CNFs occurs despite the low dispersion of the starting nickel catalyst. These results differ from those reported in the literature, in which CNF diameter was directly linked to catalyst particle size [28–30]. We discuss this discrepancy in depth in the section of this work devoted to the growth mechanism. It is noteworthy that statistical SEM analysis showed no trace of amorphous agglomerated carbon, indicating our method's high selectivity for CNF synthesis. The low formation of amorphous carbon is attributed to the synthesis temperature (680 °C), which remains quite low and hence significantly inhibits the spontaneous pyrolysis of gaseous hydrocarbon into amorphous carbon. It is also noteworthy that the synthesis temperature is closely dependent on the nature of the gaseous carbon source. For example, using a more strongly dehydrogenated carbon source (i.e., ethylene or acetylene), CNFs can be produced at lower temperatures. Note, however, that using a highly reactive hydrocarbon could also lead to the formation of thicker CNFs along with amorphous carbon.

TEM images of as-synthesized CNFs at various magnifications are presented in Fig. 4. The CNFs formed were relatively homogeneous in size [i.e., 30 nm (Fig. 4A)], with an endless length, in agreement with the SEM results reported previously. A high-magnification TEM image clearly shows the stacking of graphene planes in a fishbone structure along the fiber axis with an interplanar distance of ca. 0.34 nm, corresponding to the typically reported graphite interplanar distance (Fig. 4B). It is noteworthy that no traces of helicoidal or spiral nanofibers were observed in the sample, in contrast with the observations of Park and Keane [27]. This difference can be explained in terms of reaction temperature, the nature of the carbon source, and the hydrogen content in the feed. It seems that in our case, the nickel particles were less faceted than those formed in the experiments of Park and Keane, leading to the formation of a more homogeneous diffusion of carbon through the nickel lattice.

Fig. 5 shows a TGA diagram of the CNF/graphite composite indicating that the CNFs began to burn at 550–680 °C,

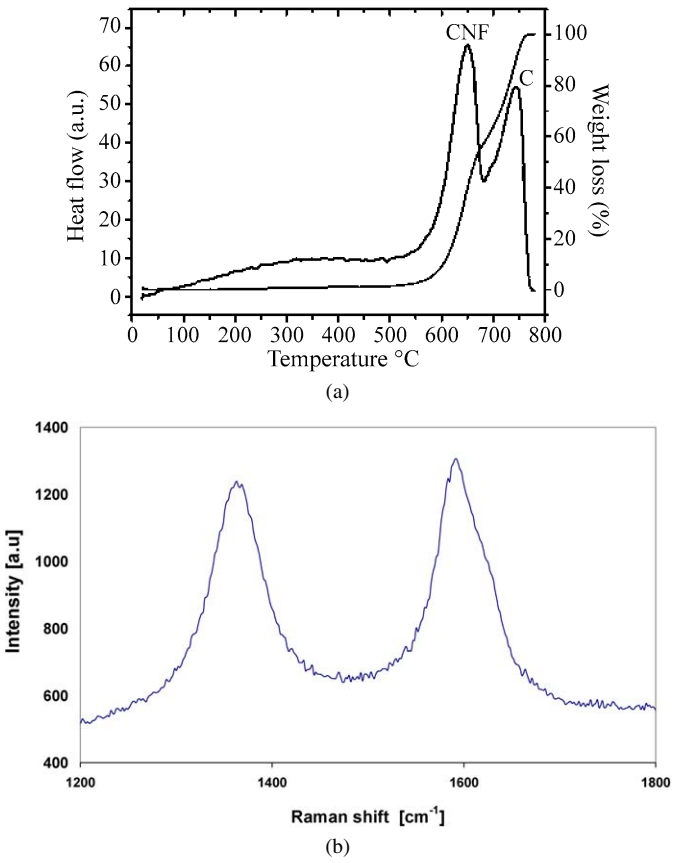

Fig. 5. (a) TGA diagram of the CNF/graphite composite. (b) Raman spectra of as-synthesized CNFs.

with the maximum centered at 650 °C. This value is between those for activated charcoal and graphite, indicating that the CNF microstructure was relatively well ordered despite the low synthesis temperature. The relatively high graphitization of the as-synthesized CNFs was confirmed by Raman spectroscopy (Fig. 5B) indicating the high surface ratio of the G-band versus the D-band.

The low-temperature (550 °C) combustion of CNFs can be directly linked to the exclusive presence of prismatic planes with higher reactivity toward oxygen. It seems that the CNF microstructure can be significantly influenced by the nature of the support. Park and Keane [27] reported similar findings from their study of how the nature of the support affects generation of CNFs by CVD. They suggested that the high degree of graphitization of the as-synthesized CNFs was due to contributions from the support as well as the presence of hydrogen in the feed. It is possible that hydrogen allows the hydrogenation of the amorphous carbon formed during the reaction and thus increases the graphitic contribution in the final material. The faceting of the nickel particle could also influence the structural order of the formed CNFs.

The formation of the CNFs on the macroscopic carbon foam contributes significantly to an increase in the final composite specific surface area from 1 to $>80\ m^2\ g^{-1}$. Taking into account that half of the solid is constituted of a low-specific surface area starting graphite foam, the actual specific surface area of the CNFs is expected to be $>160\ m^2\ g^{-1}$, in good agreement with the literature results on these systems [31]. In any case, no microporous contribution was observed, indicating the complete absence of micropores [32]. The increase in specific surface area was attributed to the extremely high external surface area (i.e., high aspect ratio of the material) of the CNFs due to the presence of graphite prismatic planes [12–14]. Similar results were previously reported for CNF composites supported on a macroscopic graphite felt [18]. However, the specific surface area of the C/C composite decreased monotonously after 2 h of CNF growth. The diminution of the specific surface area due to the formation of amorphous carbon can be rejected according to the statistical TEM observation, which demonstrates the absence of amorphous material inside the composite. The loss of surface area as a function of the duration of synthesis may be due to the branching or gathering of the CNFs onto one another, thereby diminishing accessibility to the surface of the material during gas adsorption. In prolonged synthesis some thickening of the CNFs was observed, which can contribute to the decreased specific surface area, because fibers of larger diameter present a lower external surface area. This phenomenon could be explained by the surface reconstruction of the metal catalyst that led to the formation of CNFs of larger diameter. However, this phenomenon contributes to only a relatively small extent; the gathering of the CNFs was the most important factor in the decreased overall specific surface area of the material.

3.3. Octopus growth mechanism

To gain better insight into the growth mechanism and better understanding of the discrepancy between the small CNF diameter and the relatively large metal particle size, SEM images were taken after 10 min of reaction. These images are presented in Fig. 6 with different magnifications. All CNFs are of similar diameter (i.e., 30 nm), significantly smaller than the nickel particle catalyst (i.e., 400 nm). The CNF length was relatively high, approaching several micrometers. The CNFs formed were also highly entangled, indicating the existence of numerous topological defects inside the material, because of the relatively low synthesis temperature for conventional CVD synthesis.

CNF growth seems strongly linked to the presence of peculiar faces on the nickel particle. Others have reported that the Ni(100) and Ni(110) crystalline faces are more active than the Ni(111) face for CNF growth [33]. However, the results observed in the present work seem to indicate that the final diameter of the CNFs is not dependent on the starting particle size of the growth catalyst. According to the SEM images, the CNFs are issued from several nickel faces in an octopus-like mechanism, similar to what was reported by Ermakova et al. [34] for multiwalled carbon nanotube growth over an iron-based catalyst. Fig. 6A shows the weblike network of CNFs growing from a single large nickel particle that remained attached to the graphite surface.

But our SEM analysis also showed a second growth mode from which small nickel particles were first lifted off of the support surface; subsequently, structural reconstruction leading to a second octopus-like growth mode occurred. This finding is sup-

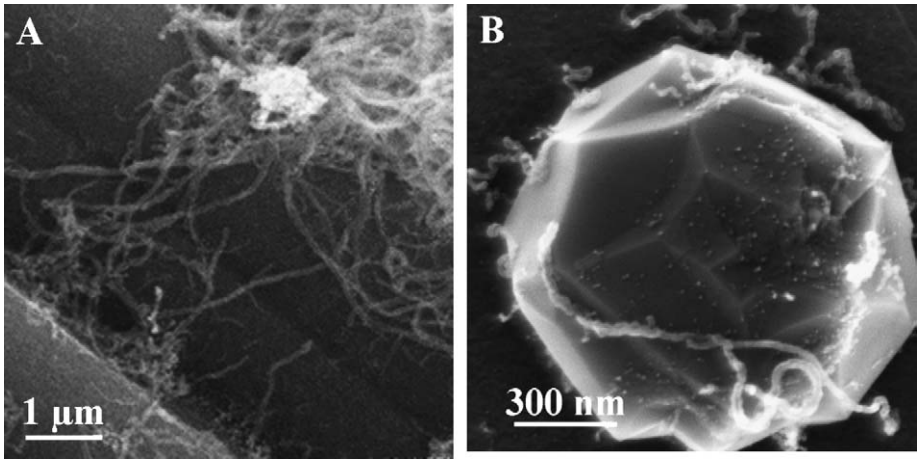

Fig. 6. The relatively long carbon nanofibers with several micrometers in length generated from a single large nickel particle (A). Base-growth mechanism where the carbon nanofibers were preferentially nucleated from specific faces of a large single nickel particle (B).

ported by the SEM images obtained at early growth states (i.e., at 2 and 10 min of reaction) (Fig. 7), which clearly show the presence of small nickel particles away from the support surface, with two CNFs growing in opposite directions (Fig. 7A). The nickel particles leaving the nickel parent aggregate are relatively homogeneous in size and relatively small (i.e., 20 to 30 nm). However, the same sample also shows an octopus-like growth of several CNFs leading to a weblike network covering the starting macroscopic shape on some nickel particles (Fig. 7B).

After 10 min of synthesis, the same observation's can be made (Figs. 7C and D). The CNF network becomes denser and the octopus-growth mode more pronounced (Fig. 7E). It is noteworthy that CNF growth at the early stages of the reaction was extremely low (i.e., diameter of ca. 10 nm). Apparently, the initially small diameter of the CNFs increased with increasing duration of synthesis.

The following growth modes are illustrated in Fig. 8: (A) a base-growth mode, in which the CNFs grow directly from a specific face of a single large nickel crystal while the other faces are responsible for the decomposition of the gaseous hydrocarbon supplying atomic carbon, and (B) a tip-like growth mode with various sequences: (i) an initial growth stage in which part of the nickel particle surface is saturated by carbon, leading to the formation of small Ni-rich carbon zone; (ii) release of the dissolved carbon to form CNFs with a concomitant lift-off of the former Ni-rich carbon particles out of the support surface and reconstruction of the nickel surface; and (iii) hydrocarbon decomposition on the new nickel faces to initiate new growth from the same particle in an octopus-like network, allowing complete coverage of the macroscopic host surface by a dense layer of CNFs.

Distinguishing the fragmentation mode of these intermediate metastable nickel carbides is difficult, however, because they are known to depend closely on the thermodynamics of the process. It is tempting to suggest that the nickel carbide was formed in an island structure instead of film according to the SEM observations showing smaller Ni particles being lifted off from larger ones.

Apparently, CNF diameter is not dependent on the initial diameter of the catalyst particle, but only on the structural modification of the starting nickel particle during the growth process. Similar results have also been reported by Emmenegger et al. [35] to explain the homogeneous diameter (i.e., 10–40 nm) of multiwalled carbon nanotubes grown from a starting continuous layer of iron oxide deposited on a planar aluminum substrate by spin coating. According to these authors, continuous catalyst particle fragmentation occurred during the course of the synthesis, leading to the formation of smaller active centers through the formation of a metastable carbide followed by its decomposition into carbon and iron particle. The existence of metastable Ni_3C during CNF formation over a MgO-supported bimetallic Ni–Cu catalyst has been reported by Zaikovskii et al. [36].

According to the relatively low interaction between the deposited nickel particles and the microfilament support, a large part of the nickel phase was present in the form of large particles (Fig. 2), which contributed mainly to an octopus-like base-growth mechanism, with only a small amount of the CNFs thus formed initiated through the tip-growth mechanism (i.e., from small nickel particles). It is noteworthy that the CNFs were extremely long (i.e., several micrometers), allowing complete coverage of the host microscopic filament surface despite the low number of growth centers.

To verify this hypothesis, a new experiment was carried out using an unsupported nickel sponge with an average particle diameter of ca. 1–3 mm instead of a supported nickel catalyst. The synthesis was performed under similar reaction conditions; Fig. 9 gives the results. The SEM images of the sample confirm the noncorrelation between the starting nickel catalyst particle size (i.e., >500 nm) and the CNF diameter (i.e., 30–40 nm), as stated earlier. The results clearly show that the diameter of the CNFs growing from nickel particles in the presence of a mixture of C_2H_6 and H_2 was completely independent of the starting catalyst particle size. It seemed that the growth centers, with diameter several times smaller than that of the starting catalyst particle, were formed during synthesis, probably via structural rearrangement of the solid solution between Ni and dissolved carbon species. The lower CNF yield obtained in the

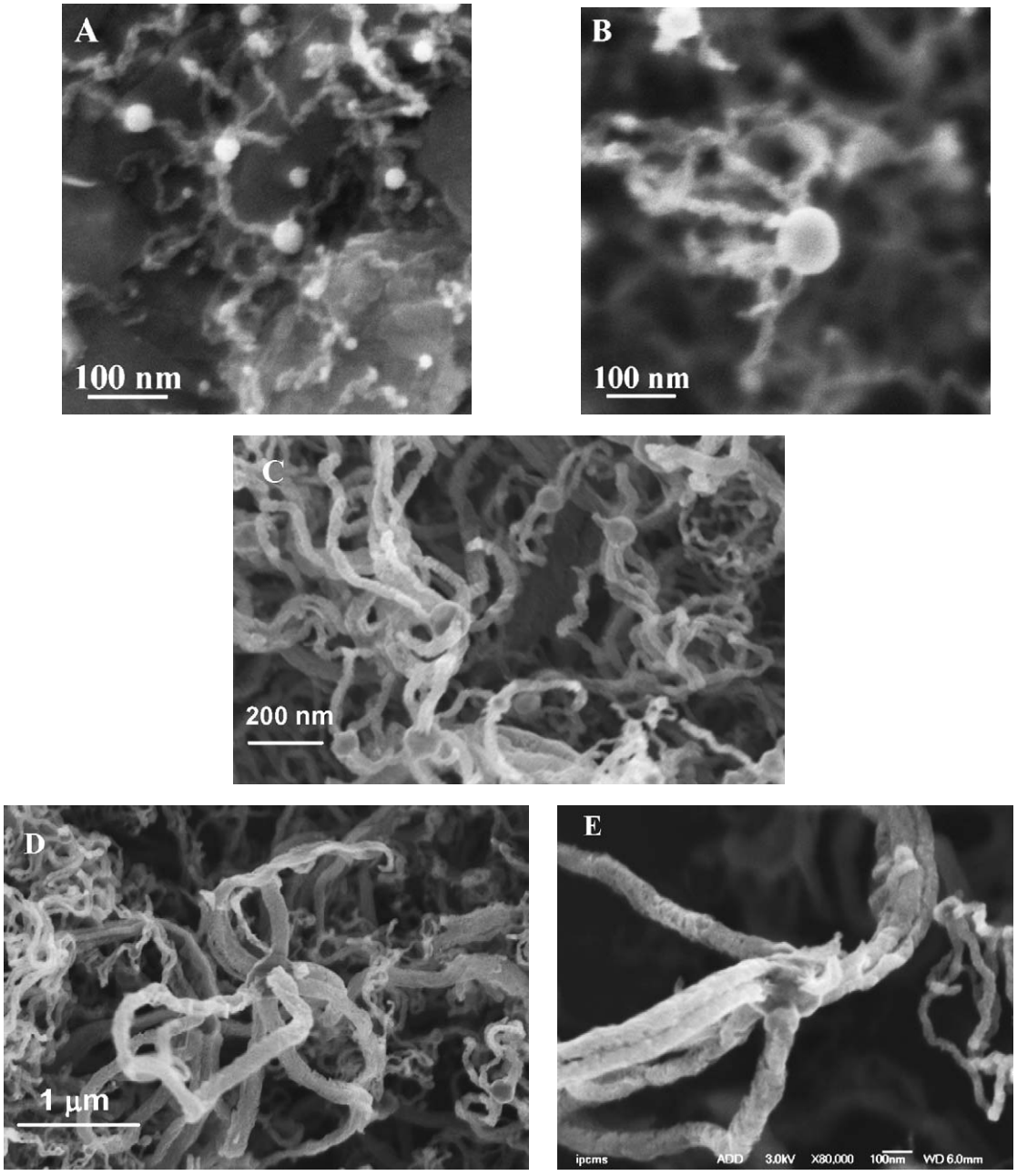

Fig. 7. SEM images of the tip-like growth process as a function of time on stream at 680 °C during the earliest stages of reaction. 2 min: (A) small nickel particles leaving from the support surface with two carbon nanofibers growing in an opposite direction. (B) Octopus-like growth observed from a single nickel particle formed from a larger nickel particle. Note the intergrowth of a single carbon nanofiber from two nickel centers. 10 min: (C) and (D) octopus-like growth observed at higher magnification (E).

bulk nickel catalyst can be attributed to the low external contact surface between the gaseous hydrocarbon source and the catalyst.

Besides producing a large amount of highly pure CNF, this work also reports one of the first studies devoted to their macroshaping for producing structured catalytic support. The shapes of the nanostructured or macrostructured C/C composites can be modified at will, depending on the intended use of these composites. Over the last decade, the use of structured reactors has become a major field in catalysis [37]. Paralleling the research devoted to find new active-phase formulations, much research has been focused on developing structured catalyst supports to improve reactor hydrodynamics and, for several reactions, catalytic performance [38–40]. The possibility of using carbon nanomaterials in catalytic processes seems to be drawing closer to realization, owing to the possibility of producing them in large quantities, thus decreasing the investment cost. Furthermore, the main drawback of these materials—their nanoscopic size, which engender both safety and hydrodynamic requirements that have hindered viable application—is now on the way to being overcome [43]. Further studies are in progress to study the kinetics of CNF growth to further optimize the composite characteristics of diameter, length, thickness, and mechanical resistance.

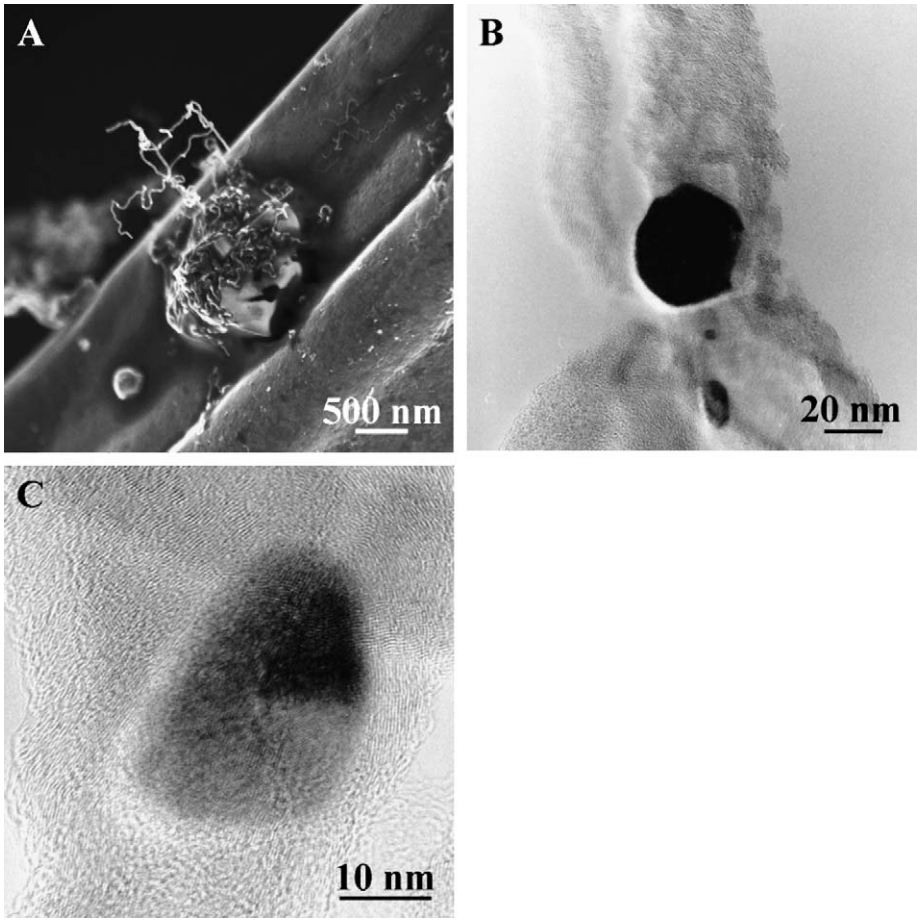

Fig. 8. Schematic growth mechanisms of carbon nanofibers over Ni supported on graphite microfilaments: (A) octopus-like base growth mechanism of the homogeneous carbon nanofibers from a relatively large nickel particle, (B) tip-like growth mechanism from a small nickel particles after lift-off from the support surface followed by an octopus-like growth mechanism (for detail see Fig. 6). (C) TEM image of the octopus-like CNF growth from a single faceted nickel particle after few minutes of reaction.

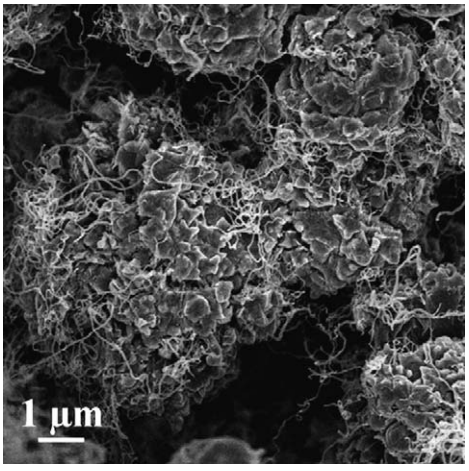

Fig. 9. Carbon nanofibers with homogeneous diameter growing from a bulk Ni sponge. The noncorrelation between the nickel particle size and the CNF diameter can be clearly seen on the SEM images.

Separate experiments carried out within the framework of the present study have shown that the average CNF diameter can be significantly controlled by altering the reaction temperature, the molar ratio of the gaseous carbon source versus hydrogen, and the nature of the metal catalyst (i.e., pure or alloyed with another metal). In the latter case, alloying nickel with copper has resulted in significantly modified CNFs in terms of both average diameter and morphology.

4. Conclusion

Graphite felt-supported nickel catalyst with relatively low metal dispersion is a highly suitable catalyst for growing CNFs with a homogeneous diameter (i.e., 30 nm) and with high yield (several hundred grams of CNF per gram of nickel) at relatively low temperature for CVD synthesis. Detailed investigations by SEM and TEM techniques have shown that the CNF diameter is completely independent of the starting nickel particle size, and several CNFs can be grown simultaneously from a large single nickel particle (i.e., >200 nm). Apparently, the CNFs grow from an octopus-like mechanism from a large nickel particle owing to the fragmentation of the nickel catalyst during the course of the synthesis, probably through metastable Ni_3C formation and decomposition. Part of the CNF formed deeply penetrated the microfilament matrix of the macroscopic host, resulting in strong mechanical stability of the final C/C composite, making it suitable for use as a catalyst support in various reactions without the formation of fine powder consecutive to the

loss of CNF by mechanical attrition. The nanoscopic structure covering the surface of the macroscopic host provides a highly accessible surface for reactants, which could significantly increase catalytic activity. The high reactivity of the prismatic planes allows better dispersion of the metal particles, contributing to the overall improvement in active site density.

Acknowledgments

The authors thank Laurie Pesant (LMSPC, UMR 7515 du CNRS) for the TPO experiments and the IPCMS (UMR 7504 du CNRS) for providing the access to their SEM and TEM facilities. R.V. thanks the CNPq (Brazil) for financial support.

References

[1] A. Chambers, T. Nemes, N.M. Rodriguez, R.T.K. Baker, J. Phys. Chem. B 102 (1998) 2251.
[2] F. Salman, C. Park, R.T.K. Baker, Catal. Today 53 (1999) 385.
[3] C. Pham-Huu, N. Keller, L. Charbonnière, R. Ziessel, M.J. Ledoux, Chem. Commun. (2000) 1871.
[4] K.P. de Jong, J.W. Geus, Catal. Rev.-Sci. Eng. 42 (2000) 481.
[5] R. Gao, C.D. Tan, R.T.K. Baker, Catal. Today 65 (2001) 19.
[6] C. Pham-Huu, N. Keller, V.V. Roddatis, G. Mestl, R. Schlögl, M.J. Ledoux, Phys. Chem. Chem. Phys. 4 (2002) 514.
[7] M.C.M. Pérez, C.S.M. de Lecea, A.L. Solano, Appl. Catal. A 151 (1997) 461.
[8] M.L. Toebes, F.F. Prinsloo, J.H. Bitter, A.J. van Dillen, K.P. de Jong, Stud. Surf. Sci. Catal. 143 (2002) 201.
[9] S.R. de Miguel, J.I. Vilella, E.L. Jablonski, O.A. Scelza, C.S.M. de Lecea, A.L. Solano, Appl. Catal. A 232 (2002) 237.
[10] J.M. Nhut, R. Vieira, L. Pesant, J.P. Tessonnier, N. Keller, G. Ehret, C. Pham-Huu, M.J. Ledoux, Catal. Today 76 (2002) 11.
[11] S.F. Yin, Q.H. Zhang, B.Q. Xu, W.X. Zhu, C.F. Ng, C.T. Au, J. Catal. 224 (2004) 384.
[12] R. Vieira, M.J. Ledoux, C. Pham-Huu, Appl. Catal. A 274 (2004) 1.
[13] C. Pham-Huu, N. Keller, G. Ehret, L. Charbonnière, R. Ziessel, M.J. Ledoux, J. Mol. Catal. A 170 (2001) 155.
[14] N.M. Rodriguez, M.S. Kim, R.T.K. Baker, J. Phys. Chem. 98 (1994) 108.
[15] J.M. Planeix, N. Coustel, B. Coq, V. Brotons, P.S. Kumbhar, R. Dutartre, P. Geneste, P. Bernier, P.M. Ajayan, J. Am. Chem. Soc. 116 (1994) 7935.
[16] B.L. Mojet, M.S. Hoogenraad, A.J. van Dillen, J.W. Geus, D.C. Koningsberger, J. Chem. Soc., Faraday Trans. 93 (1997) 4371.
[17] C. Pham-Huu, R. Vieira, L. Charbonnière, R. Ziessel, M.J. Ledoux, French Pat. Appl. No. 01-15178, assigned to SICAT SA, 2001.
[18] R. Vieira, C. Pham-Huu, N. Keller, M.J. Ledoux, Chem. Commun. (2002) 954.
[19] M.L. Toebes, F.F. Prinsloo, J.H. Bitter, A.J. van Dillen, K.P. de Jong, J. Catal. 214 (2003) 78.
[20] R.T.K. Baker, P.S. Harris, R.B. Thomas, R.J. Waite, J. Catal. 30 (1973) 86.
[21] R.L. Van der Wal, L.J. Hall, Carbon 41 (2003) 659.
[22] C. Park, M.A. Keane, J. Catal. 221 (2003) 386.
[23] C. Park, R.T.K. Baker, J. Phys. Chem. B 102 (1998) 5168.
[24] C. Park, R.T.K. Baker, J. Catal. 179 (1998) 361.
[25] D.R. Rainer, D.W. Goodman, J. Mol. Catal. A 131 (1998) 259.
[26] J.M. Ting, R.M. Liu, Carbon 41 (2003) 601.
[27] C. Park, M.A. Keane, J. Catal. 221 (2004) 386.
[28] S.B. Sinnott, R. Andrews, D. Qian, A.M. Rao, Z. Mao, E.C. Dickey, F. Derbyshire, Chem. Phys. Lett. 315 (1999) 25.
[29] J.F. Colomer, C. Stephan, S. Lefrant, G. van Tendeloo, I. Willems, Z. Konya, A. Fonseca, Ch. Laurent, J.B. Nagy, Chem. Phys. Lett. 317 (2000) 83.
[30] M.L. Toebes, J.H. Bitter, A.J. van Dillen, K.P. de Jong, Catal. Today 76 (2002) 33.
[31] P. Serp, M. Corrias, P. Kalck, Appl. Catal. A 253 (2003) 337.
[32] M.J. Ledoux, R. Vieira, C. Pham-Huu, N. Keller, J. Catal. 216 (2003) 333.
[33] I. Alstrup, J. Catal. 109 (1988) 241.
[34] M.A. Ermakova, D.Yu. Ermakov, A.L. Chuvilin, G.G. Kuvshinov, J. Catal. 201 (2001) 183.
[35] C. Emmenegger, J.M. Bonard, P. Mauron, P. Sudan, A. Lepora, B. Grobety, A. Züttel, L. Schlapbach, Carbon 41 (2003) 539.
[36] V.I. Zaikovskii, V.V. Chesnokov, R.A. Buyanov, Kinet. Catal. 40 (1999) 612.
[37] A. Cybulski, J.A. Moulijn, Structured Catalysts and Reactors, Marcel Dekker, New York, 1998.
[38] H.P. Calis, A.W. Gerritsen, C.M. van den Bleek, C.H. Legein, J.C. Jansen, H. van Bekkum, Can. J. Chem. Eng. 73 (1995) 120.
[39] B. Louis, L. Kiwi-Minsker, P. Reuse, A. Renken, Ind. Eng. Chem. Res. 40 (2001) 1454.
[40] M.J. Ledoux, C. Pham-Huu, Catal. Today 102–103 (2005) 2.
[41] S. Iijima, Nature 354 (1991) 56.
[42] P.E. Nolan, D.C. Lynch, A.H. Cutler, J. Phys. Chem. B 102 (1998) 4165.
[43] M.K. van der Lee, A.J. van Dillen, J.W. Geus, K.P. de Jong, J.H. Bitter, Carbon 44 (2006) 629.
[44] N.A. Jarrah, F. Li, J.G. van Ommen, L. Lefferts, J. Mater. Chem. 15 (2005) 1946.